applied sciences

MDPI

Article

Vibrational Model of Heat Conduction in a Fluid of Hard Spheres

Sergey Khrapak

Joint Institute for High Temperatures, Russian Academy of Sciences, 125412 Moscow, Russia; sergey.khrapak@gmx.de

Abstract: Application of a vibrational model of heat transfer to a fluid made of hard spheres is discussed. The model was originally proposed to describe heat conduction in fluids with soft pairwise interactionsHere, it is shown that only minor modifications are required to apply the model in the opposite limit of hard sphere interactions. Good agreement with recent results from molecular dynamics simulation is documented in the moderately dense regime. Near the freezing point, however, the model overestimates the thermal conductivity coefficient (by $\simeq$50%). The new approach is compared with other simple models for the thermal conductivity coefficients such as Bridgman's expression and the Enskog formula. The value of the coefficient in the Bridgman's expression, appropriate for the hard sphere fluid, is determined. A new expression for the dependence of the reduced thermal conductivity coefficient on the reduced excess entropy is proposed. The obtained results can be useful for rough estimates of the thermal conductivity coefficient of simple fluids with steep interactions when more accurate experimental results are not available.

Keywords: transport properties of fluids; heat conduction; hard sphere fluid; vibrational mechanism of atomic transport; collective modes

Citation: Khrapak, S. Vibrational MOdel of Heat Conduction in a Fluid of Hard Spheres. *Appl. Sci.* **2022**, *12*, 7939. https://doi.org/10.3390/app12157939

Academic Editors: Ştefan Ţălu and Mihai Ţălu

Received: 9 July 2022
Accepted: 2 August 2022
Published: 8 August 2022

1. Introduction

Our understanding of dynamical and transport properties of liquids remains incomplete and fragmented even in the case of the simplest atomic systems. Despite considerable progress achieved over the years [1–6], we still often need to apply various phenomenological approaches, semi-quantitative models, and scaling relations. Among the renowned examples are the Stokes-Einstein relation between the self-diffusion and the shear viscosity coefficients [4,7–17], the excess entropy scaling of reduced transport coefficients [18–22], and several variants of the freezing temperature scaling [23–27]. Recently, a freezing density scaling of reduced transport coefficients of the Lennard-Jones and related fluids has been discussed as a new useful addition to the existing approaches [28–30].

Heat transfer in fluids (throughout this paper the term "fluid" is applied to liquids and supercritical fluids) is an important topic of contemporary research with diverse interdisciplinary applications [31–36]. A vibrational model of heat transfer has been recently applied to fluids with soft pairwise interactions [37] . In this model, the thermal conductivity coefficient is proportional to the effective frequency of atomic vibrations around the local temporary equilibrium positions. The effective frequency is related to the properties of the liquid collective excitation spectrum. The model has been applied to quantify heat transfer in a strongly coupled one-component plasma fluid, dense Lennard-Jones liquid, and plasma-related screened Coulomb (Yukawa) fluid. An impressive agreement with the available results from numerical simulations has been documented [37–39]. The purpose of this work is to consider the applicability of the vibrational model to a new physical system—a fluid made of hard spheres (HS fluid). The vibrational picture of atomic dynamics is clearly not very appropriate for extremely anharmonic HS system. Nevertheless, collective excitations are supported in the dense HS fluid and averaging over collective modes can formally

be performed. The question is whether the results have any relation to reality. It will be shown below that a formal expression based on the vibrational model of heat transfer is in agreement with the results from molecular dynamics simulations in a moderately dense regime, but overestimates the numerical results near the freezing point. The accuracy of some other simplistic approaches will be also examined. In particular, the coefficient in the Bridgman's expression, appropriate for the HS fluid, will be identified. The excess entropy scaling of the thermal conductivity coefficient in the HS fluid will be briefly discussed and a new expression will be proposed. The results can be useful for simple rough theoretical estimates when more accurate data are unavailable.

2. Hard Sphere Fluid

The HS interaction potential is defined as:

$$\phi(r) = \begin{cases} \infty, & r < \sigma \\ 0, & r \geq \sigma, \end{cases} \tag{1}$$

where σ is the sphere diameter and r is the distance between the centres of two spheres. The potential ensures that spheres cannot overlap. The HS system is a very important simple model for the properties of condensed matter in its various states [40–47].

The thermodynamic and transport properties of HS systems depend on a single reduced density parameter, $\rho^* = \rho\sigma^3$, or the packing fraction, $\eta = \pi\rho\sigma^3/6$, where ρ is the density. Transport properties of the HS fluid have been extensively studied (see e.g., Ref. [42] for a review). Here we use recent molecular dynamics (MD) simulation results for the thermal conductivity coefficient reported by Pieprzyk et al. [48]. The use of large simulation systems and long simulation times allowed accurate prediction of the thermal conductivity coefficient in the thermodynamic limit.

Throughout the paper we use macroscopically reduced units for the thermal conductivity coefficient:

$$\lambda_R = \lambda \frac{\rho^{-2/3}}{v_T}, \tag{2}$$

where λ is the dimensional thermal conductivity coefficients, $v_T = \sqrt{T/m}$ is the thermal velocity, T is the temperature in energy units ($\equiv k_B T$), and m is the atomic mass. This normalization is essential in Rosenfeld's excess entropy scaling approach [18,19], therefore the subscript R is often used. This normalization does not contain the Boltzmann constant k_B, because the temperature is measured in energy units. Another normalization that is commonly employed is:

$$\lambda^* = \lambda \frac{\sigma^2}{v_T}. \tag{3}$$

These two normalizations are related via $\lambda^* = \lambda_R(\rho^*)^2$.

3. Vibrational Model

The vibrational paradigm of atomic dynamics in dense liquids has been discussed by many authors over the years, see e.g., Refs. [1,7,49–51]. The main assumptions involved are as follows [16]: Atoms exhibit solid-like oscillations about temporary equilibrium positions corresponding to a local minimum on the system's potential energy surface [1,51]. These positions do not form a regular lattice like in crystalline solids, but correspond to a liquid-like structure [50]. They are also not fixed and change (diffuse or drift) with time, which allows liquids to flow. However, these rearrangements occur on much longer time scales than those characterising solid-like oscillations. Effectively, one can assume that the local configurations of atoms are preserved for some time until a fluctuation in the kinetic energy allows the positions of some of these atoms to be rearranged towards a new local minimum in the multidimensional potential energy surface. This picture allows to make important approximations about the properties of atomic motion and the mechanisms

of momentum and energy transport in the liquid state. For instance, the Stokes-Einstein (SE) relation without the hydrodynamic radius naturally emerges within this vibrational paradigm under a few additional assumptions [7,13,15,16].

For energy transfer, separation of time scales corresponding to fast solid-like atomic oscillations and their slow drift plays a dominant role. Namely, it is reasonable to assume that a vibrating atom transports energy from its hotter to its cooler neighbors with a characteristic energy exchange rate equal to its average vibrational frequency, $\nu = \langle\omega\rangle/2\pi$. Each atom controls the energy transfer through an area of order Δ^2, where $\Delta = \rho^{-1/3}$ is the average interatomic separation. A liquid can be approximated by a quasi-layered structure with quasi-layers that are perpendicular to the temperature gradient (applied along x-axis) and are separated by the distance Δ (see e.g., Figure 1 from Ref. [37]). The energy difference between two neighbouring layers is $(dU/dx)\Delta$. The energy flux density can be approximated as:

$$j \simeq -\frac{\nu}{\Delta^2}\left(\frac{dU}{dx}\right)\Delta = -\frac{\langle\omega\rangle}{2\pi\Delta}c_{\mathrm{p}}\frac{dT}{dx}, \tag{4}$$

where $c_{\mathrm{p}} = (dU/dT)_{\mathrm{p}}$ is the specific heat at constant pressure and the minus sign implies that the heat flow is down the temperature gradient. On the other hand, Fourier's law of the heat transfer reads:

$$j = -\lambda\frac{dT}{dx}. \tag{5}$$

By comparing Equations (4) and (5) we immediately obtain:

$$\lambda = c_{\mathrm{p}}\frac{\langle\omega\rangle}{2\pi\Delta}. \tag{6}$$

This is essentially the expression derived in Ref. [37], except that the specific heat at constant volume, c_{v}, appeared there. The present choice seems in general more appropriate because pressure should be constant in equilibrium. The difference is insignificant for soft spheres, because dense fluids can be considered as essentially incompressible in a wide portion of their phase diagram not too far from the freezing curve and thus $c_{\mathrm{p}} \simeq c_{\mathrm{v}}$ holds. For example, Equation (6) with $c_{\mathrm{p}} \to c_{\mathrm{v}}$ works very well for soft plasma-related Coulomb and Yukawa interactions and the Lennard-Jones fluid [37–39]. In such cases it is more appropriate to use c_{v} for practical estimates (since c_{v} is normally easier to evaluate). This is not the case, however, in the HS limit. For hard spheres $c_{\mathrm{v}} \equiv 1.5$ and c_{p} and c_{v} can differ very considerably.

Before we discuss heat conduction further, it should be emphasized that the vibrational picture of atomic dynamics is not particularly suitable for the HS fluid. In contrast to softer interactions, atomic motion does not exhibit a pronounced oscillatory character [52–54]. The HS fluid is extremely anharmonic and dynamics is dominated by short hard-core-like collision events [55]. Nevertheless, similar to other simple fluids, the dense HS fluid does support the longitudinal and transverse collective excitations [56] (with a forbidden long-wavelength region for the transverse mode, the so-called "k-gap" [56–60]). Therefore, averaging over collective modes can be performed and in this sense $\langle\omega\rangle$ remains a meaningful quantity. The Stokes-Einstein relation holds in the HS fluid, just as it does in soft sphere fluids, where it emerges naturally as a consequence of the vibrational picture of atomic dynamics [7,16]. Vibrational model allows to estimate the excess entropy of various fluids with pairwise repulsive interactions near the fluid–solid phase transition, including the HS limit [61]. Under these circumstances it is not very unreasonable to compare the predictions of Equation (6) with the available results from MD simulations in the HS limit.

Since the actual frequency distribution is often not known in liquids, and can vary from one type of liquid to another, some simplifying assumptions are necessary to evaluate $\langle\omega\rangle$ in Equation (6). In the simplest Einstein approximation all atoms vibrate with the same (Einstein) frequency Ω_{E}. We arrive at the expression derived by Horrocks and

McLaughlin [62]. But this approximation is obviously not applicable to the HS fluid. The conventional expression for the Einstein frequency,

$$\Omega_{\mathrm{E}} = \frac{\rho}{3m} \int d\mathbf{r} \nabla^2 \phi(r) g(r), \tag{7}$$

where $g(r)$ is the radial distribution function (RDF), is simply undefined in the HS limit.

One can use an acoustic spectrum, $\omega = kc_s$ with an appropriate maximum cutoff wavenumber $k_{\max}$. Here c_s is the conventional adiabatic sound velocity. Then, the standard averaging procedure would result in:

$$\lambda \sim \frac{c_s}{\Delta^2}. \tag{8}$$

This can be considered as an analog of Bridgman's equation [63]. The numerical coefficient remains undefined, because of the qualitative character of the arguments involved (the values between 2 and 3 can be found in the literature, see e.g., Ref. [35]). We shall see that for the HS fluid the numerical coefficient is in fact close to unity.

As a more physically sound approximation, assume that a dense liquid supports one longitudinal and two transverse collective modes. Debye-like averaging in k-space can be performed using acoustic asymptotes $\omega_l(k) = c_l k$ and $\omega_t(k) = c_t k$ in the long-wavelength domain, where c_l and c_t are the longitudinal and transverse sound velocities, respectively. The thermal conductivity coefficient becomes [37]:

$$\lambda \simeq \frac{1}{4} \left(\frac{3}{4\pi} \right)^{1/3} c_{\mathrm{p}} \frac{c_l + 2c_t}{\Delta^2}. \tag{9}$$

If we substitute $c_{\mathrm{p}} \simeq c_{\mathrm{v}} \simeq 3$ near the freezing point (according to Dulong-Petit law), we get a formula, which is similar to that of the minimal thermal conductivity model proposed by Cahill and Pohl for amorphous solids [64–66]. It turns out that a similar formula obtained using the vibrational model works rather well in the liquid regime. It is the expression (9) that will be compared with the recent MD data on the thermal conductivity coefficient of the HS fluid. Note that there are no free parameters in the discussed approach.

4. Methods

To evaluate the thermal conductivity coefficient from Equation (9) we need to know the longitudinal and transverse sound velocities (c_l and c_t) and the specific heat at constant pressure (c_{p}). The later is obtained from the equation of state of the HS fluid. Here a simple but sufficiently accurate equation of Carnahan and Starling (CS) is used [67]. The pressure is written as:

$$P(\rho, T) = \rho T Z(\eta), \qquad Z(\eta) = \frac{1 + \eta + \eta^2 - \eta^3}{(1-\eta)^3}, \tag{10}$$

where $Z(\eta)$ is the CS compressibility.

The various sound velocities are related to the elastic moduli. For example, the adiabatic sound velocity c_s is related to the adiabatic bulk modulus K_s via $c_s = \sqrt{K_s/m\rho}$. The adiabatic bulk modulus K_s is determined from the CS compressibility factor Z [68,69]:

$$K_s = \rho T \left[Z(\eta) + \eta dZ(\eta)/d\eta + \tfrac{2}{3} Z^2(\eta) \right]. \tag{11}$$

Similarly, the longitudinal and transverse sound velocities are obtained from the longitudinal and transverse instantaneous (infinite frequency) elastic moduli, $c_l = \sqrt{M_\infty/m\rho}$ and $c_t = \sqrt{G_\infty/m\rho}$. Moreover, the longitudinal elastic modulus is related to the bulk and shear moduli via:

$$M_\infty = K_\infty + \tfrac{4}{3} G_\infty. \tag{12}$$

The behavior of elastic moduli when approaching the HS interaction limit has recently been discussed in detail [60]. For the instantaneous shear and bulk moduli, the expressions derived by Miller [70] are employed, with minor modifications discussed in Ref. [71]. The shear modulus is [70,71]:

$$G_\infty = \rho T\left[1 - \frac{8}{5}\eta g'(1)\right], \tag{13}$$

where $g'(1)$ denotes the reduced derivative at contact, $g'(1) = \lim_{\epsilon\to 0}[dg(x)/dx]_{x=1+\epsilon}$ with $x = r/\sigma$. For $g'(1)$ we use the approximation proposed in Ref. [72]:

$$g'(1) = -\frac{9\eta(1+\eta)}{2(1-\eta)^4}. \tag{14}$$

The bulk modulus is [70,71]:

$$K_\infty = 2P - \frac{8}{3}\rho T + \frac{2}{3}\frac{P^2}{\rho T} + \frac{5}{3}G_\infty. \tag{15}$$

The longitudinal modulus is then obtained from Equation (12). This allows to evaluate all necessary quantities and compare the results of various approaches with those from MD simulations. Results are reported in the next Section.

5. Results

Figure 1 shows the comparison between the MD data on the reduced thermal conductivity coefficient and the discussed theoretical approximations. Symbols correspond to the MD data [48]. The quantitative picture is conventional and resembles that in other simple fluids, see e.g., Refs. [30,73]. In the low-density domain λ_R decreases with density. In the first approximation, the thermal conductivity coefficient of a dilute HS gas is $\lambda_0 = (75/64\sigma^2)(T/\pi m)^{1/2}$ [74], which leads to $\lambda_R \simeq 0.661/(\rho^*)^{2/3}$ [28]. The minimum of λ_R is reached at $\rho^* \simeq 0.25$. The amplitude of this minimum is known to be quasi-universal for many model and real fluids. Numerically, a rough estimte $\lambda_R^{\min} \sim 3$ holds for various liquids, except for plasma-related fluids with very soft Coulomb-like interactions [30,73]. This minimum corresponds to the crossover between two different mechanisms of energy transfer: pairwise collisions in the dilute gas regime and collective vibrations in the dense fluid regime. Note that a similar minimum appears in the reduced viscosity coefficient [30,73]. It is the location of the reduced viscosity minimum that previously served as one of the definitions of the gas-liquid dynamical crossover [75,76]. After the minimum, λ_R increases monotonously with density. The typical value of the thermal conductivity coefficient at the freezing point of various simple liquids is $\lambda_R^{\rm fr} \sim 10$ [30,73]. We observe in Figure 1 that the thermal conductivity coefficient of the HS fluid at the freezing point is around $\simeq 30\%$ higher. A similar observation was previously made in Ref. [28].

The dashed curve in Figure 1 corresponds to the vibrational model of heat transfer as formulated above. The agreement is reasonably good at moderate densities (after minimum in λ_R is reached), but becomes worse at $\rho^* \gtrsim 0.7$. As the freezing density ($\rho^*_{\rm fr} \simeq 0.939$ according to Ref. [77]) is approached the vibrational model overestimates λ_R by $\simeq 50\%$. This reflects the fact that the vibrational picture is not very appropriate for the dense HS fluid. It is to some extent surprising that the expression based on the averaging over collective modes remains a relatively good approximation in the moderately dense regime.

The dash-dotted curve corresponds to the Bridgman's expression. Plotted is the value $\lambda_R = c_s/v_T$, where c_s is evaluated using Equation (11). We see that the numerical factor equal to unity is appropriate for the dense HS fluid. Only near the freezing point it leads to some underestimation of λ_R.

The solid curve corresponds to the Enskog theory, which is an extension of the gas kinetic theory for the transport coefficients to finite densities. It accounts for the excluded volume effects, but assumes that the successive collisions between the atoms are uncor-

related. The Enskog expression for the thermal conductivity coefficient of the HS fluid reads [48]:

$$\lambda = 1.02513\lambda_0\rho B_2\left(\frac{1}{Z_{ex}} + 1.2 + 0.7574Z_{ex}\right), \tag{16}$$

where λ_0 is the first approximation for λ in the infinitely dilute gaseous limit (see above), the coefficient 1.02513 is the Sonine polynomial correction up to 4th term, $B_2 = 2\pi\sigma^3/3$ is the second virial coefficient, and $Z_{ex} = Z - 1$ is the excess compressibility factor. It is observed that overall the thermal conductivity coefficient of the HS fluid is rather well described by the Enskog theory. Deviations from MD data of Ref. [48] do not exceed ∼5% in the entire fluid regime. This is in contrast to other transport properties: Agreement with Enskog theory for the self-diffusion and viscosity coefficients only takes place at sufficiently low densities [77].

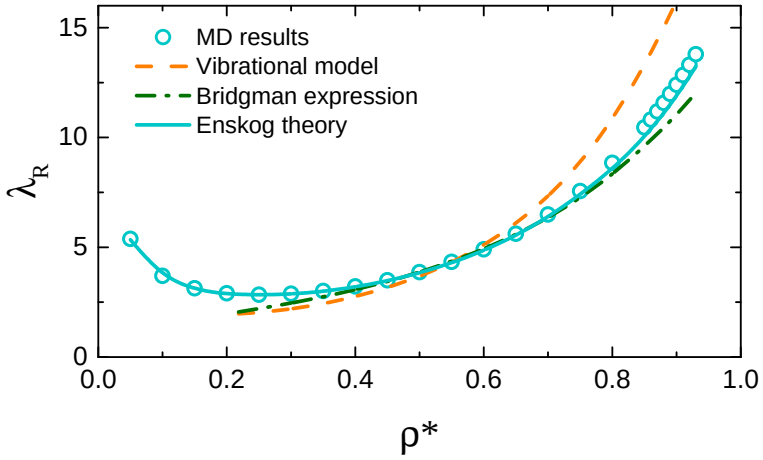

Figure 1. (Color online) Macroscopically reduced thermal conductivity coefficient λ_R of the HS fluid as a function of the reduced density ρ^*. Symbols correspond to the numerical results from Ref. [48]. The dashed curve denotes the calculation using the vibrational model, the dash-dotted curve corresponds to the Bridgman's expression, and the solid curve is plotted using the Enskog theory.

6. Excess Entropy Scaling

In view of the importance of the excess entropy scaling for transport coefficients in fluids, the reduced thermal conductivity λ_R is replotted in Figure 2 as a function of the excess entropy. Excess entropy is defined as the actual entropy minus the entropy of an ideal gas at the same temperature and density, divided by the number of particles and Boltzmann constant k_B to make it dimensionless. It is negative in fluids, because they are more ordered than the ideal gas. The excess entropy can be easily calculated using the CS compressibility:

$$s_{ex} = \int_0^\eta \frac{1 - Z(\eta)}{\eta} d\eta = \frac{\eta(3\eta - 4)}{(1-\eta)^2}. \tag{17}$$

In Figure 2 symbols are the MD numerical results from Ref. [48]. The dashed curve corresponds to a "quasi-universal" exponential scaling proposed by Rosenfeld, $\lambda_R \sim 1.5\exp(-0.5s_{ex})$ [19]. The advantage of this scaling is that it allows to estimate reasonably well (within about $\simeq 30\%$) the thermal conductivity coefficient in various systems with quite disparate pair interactions [19]. On the other hand, different potentials can be fitted better by somewhat different functional forms (see e.g., Ref. [22]). For the HS fluid we propose a simple cubic polynomial fit of the form

$$\lambda_R = 2.3845 + 0.0272s_{ex} + 0.6550s_{ex}^2 - 0.0307s_{ex}^3. \tag{18}$$

This fit does a very good job for $s_{ex} \lesssim -1$, as shown by the solid curve in Figure 2.

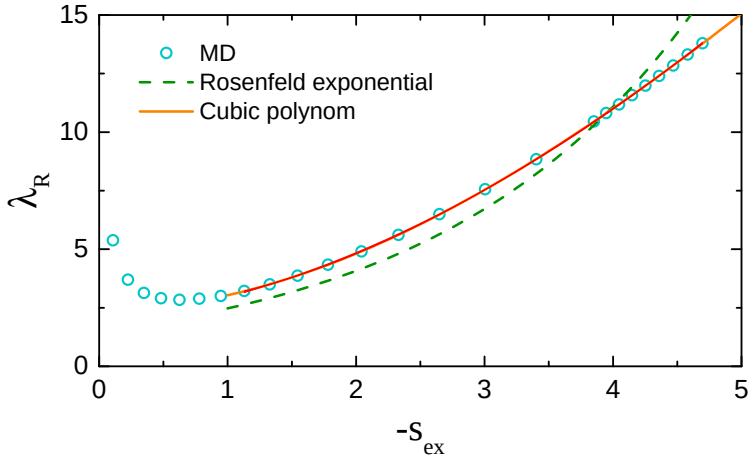

Figure 2. (Color online) Macroscopically reduced thermal conductivity coefficient λ_R of the HS fluid as a function of the negative excess entropy $-s_{ex}$. Symbols correspond to the numerical results from Ref. [48]. The dashed curve is the "quasi-universal" exponential scaling proposed by Rosenfeld. The solid curve is a cubic polynomial fit.

7. Conclusions

The system composed of hard spheres is a very important model in statistical mechanics and condensed matter physics. It allows to understand many generic mechanisms behind quasi-universal structural and dynamical properties of real materials. In this paper we discussed the properties of thermal conduction in the HS fluid. It has been demonstrated that the expression obtained within the vibrational model of atomic transport provides a reasonable description of the thermal conductivity coefficient at moderate densities, but leads to a significant overestimation (up to $\simeq$50%) near the freezing point. Overall, this is not particularly surprising, because the extremely anharmonic HS system does not fit into the vibrational paradigm and the vibrational model was not originally intended for the HS fluid. On the other hand, it should be noted that the Stokes-Einsten relation, emerging naturally within the vibrational paradigm of atomic transport, is satisfied to a good accuracy in the dense HS fluid. The vibrational model allows to estimate the excess entropy for fluids with repulsive interactions, including the HS limit. Thus, the vibrational approach seems not completely irrelevant and this represents an important lesson from this study. We have also demonstrated that the reduced thermal conductivity coefficient correlates well with the reduced sound velocity, and the Bridgman's expression applies. The coefficient of proportionality is close to unity, much smaller than usually quoted. The Enskog expression is known to work rather well in the entire HS fluid density range, but it is not directly applicable to other system as the vibrational model does. Yet, the vibrational model is clearly much better suited for soft pairwise interactions.

Funding: This research received no external funding.

Institutional Review Board Statement: Not applicable.

Informed Consent Statement: Not applicable.

Data Availability Statement: Not applicable.

Conflicts of Interest: The author declares no conflict of interest.

Abbreviations

The following abbreviations are used in this manuscript:

HS Hard Sphere
CS Carnahan and Starling

MD	Molecular Dynamics
RDF	Radial distribution function

Nomenclature

B_2	second virial coefficient
c_s	adiabatic sound velocity
c_l	longitudinal instantaneous sound velocity
c_t	transverse instantaneous sound velocity
c_p	specific heat at constant pressure
c_v	specific heat at constant volume
$g(r)$	radial distribution function (RDF)
G_∞	instantaneous (infinite frequency) shear modulus
j	energy flux density
K_s	adiabatic bulk modulus
K_∞	instantaneous (infinite frequency) bulk modulus
m	mass of an atom (particle)
M_∞	instantaneous (infinite frequency) longitudinal modulus
P	pressure
s_ex	reduced excess entropy
T	temperature (in energy units)
U	internal energy
$v_\mathrm{T} = \sqrt{T/m}$	thermal velocity
$Z = P/\rho T$	compressibility factor
$Z_\mathrm{ex} = Z - 1$	excess compressibility factor
$\Delta = \rho^{-1/3}$	average interatomic separation
$\eta = \pi\rho\sigma^3/6$	packing fraction
λ	thermal conductivity coefficient
λ_R	reduced thermal conductivity coefficient
ρ	density
$\rho^* = \rho\sigma^3$	reduced density
σ	hard sphere diameter
$\phi(r)$	pairwise interaction potential
Ω_E	Einstein frequency

References

1. Frenkel, Y. *Kinetic Theory of Liquids*; Dover: New York, NY, USA, 1955.
2. Barker, J.A.; Henderson, D. What is "liquid"? Understanding the states of matter. *Rev. Mod. Phys.* **1976**, *48*, 587–671. [CrossRef]
3. Groot, S.R.; Mazur, P. *Non-Equilibrium Thermodynamics*; Courier Corporation: New York, NY, USA, 1984.
4. Balucani, U.; Zoppi, M. *Dynamics of the Liquid State*; Clarendon Press: Oxford, UK, 1994.
5. March, N.H.; Tosi, M.P. *Introduction to Liquid State Physics*; World Scientific Pub Co Inc.: Singapore, 2002.
6. Hansen, J.P.; McDonald, I.R. *Theory of Simple Liquids*; Elsevier: Amsterdam, The Netherlands, 2006.
7. Zwanzig, R. On the relation between self-diffusion and viscosity of liquids. *J. Chem. Phys.* **1983**, *79*, 4507–4508. [CrossRef]
8. Balucani, U.; Vallauri, R.; Gaskell, T. Generalized Stokes-Einstein Relation. *Ber. Der Bunsenges. Phys. Chem.* **1990**, *94*, 261–264. [CrossRef]
9. Ohtori, N.; Ishii, Y. Explicit expression for the Stokes-Einstein relation for pure Lennard-Jones liquids. *Phys. Rev. E* **2015**, *91*, 012111. [CrossRef]
10. Ohtori, N.; Miyamoto, S.; Ishii, Y. Breakdown of the Stokes-Einstein relation in pure Lennard-Jones fluids: From gas to liquid via supercritical states. *Phys. Rev. E* **2017**, *95*, 052122. [CrossRef]
11. Ohtori, N.; Uchiyama, H.; Ishii, Y. The Stokes-Einstein relation for simple fluids: From hard-sphere to Lennard-Jones via WCA potentials. *J. Chem. Phys.* **2018**, *149*, 214501. [CrossRef]
12. Costigliola, L.; Heyes, D.M.; Schrøder, T.B.; Dyre, J.C. Revisiting the Stokes-Einstein relation without a hydrodynamic diameter. *J. Chem. Phys.* **2019**, *150*, 021101. [CrossRef]
13. Khrapak, S. Stokes–Einstein relation in simple fluids revisited. *Mol. Phys.* **2019**, *118*, e1643045. [CrossRef]
14. Ohtori, N.; Kondo, Y.; Shintani, K.; Murakami, T.; Nobuta, T.; Ishii, Y. The Stokes-Einstein Relation for Non-spherical Molecular Liquids. *Chem. Lett.* **2020**, *49*, 379–382. [CrossRef]
15. Khrapak, S.A.; Khrapak, A.G. Excess entropy and Stokes-Einstein relation in simple fluids. *Phys. Rev. E* **2021**, *104*, 044110. [CrossRef]

16. Khrapak, S.A. Self-Diffusion in Simple Liquids as a Random Walk Process. *Molecules* **2021**, *26*, 7499. [CrossRef] [PubMed]
17. Khrapak, S. Diffusion, viscosity, and Stokes-Einstein relation in dense supercritical methane. *J. Mol. Liq.* **2022**, *354*, 118840. [CrossRef]
18. Rosenfeld, Y. Relation between the transport coefficients and the internal entropy of simple systems. *Phys. Rev. A* **1977**, *15*, 2545–2549. [CrossRef]
19. Rosenfeld, Y. A quasi-universal scaling law for atomic transport in simple fluids. *J. Phys. Condens. Matter* **1999**, *11*, 5415–5427. [CrossRef]
20. Dzugutov, M. A universal scaling law for atomic diffusion in condensed matter. *Nature* **1996**, *381*, 137–139. [CrossRef]
21. Dyre, J.C. Perspective: Excess-entropy scaling. *J. Chem. Phys.* **2018**, *149*, 210901. [CrossRef]
22. Bell, I.H.; Messerly, R.; Thol, M.; Costigliola, L.; Dyre, J.C. Modified Entropy Scaling of the Transport Properties of the Lennard-Jones Fluid. *J. Phys. Chem. B* **2019**, *123*, 6345–6363. [CrossRef]
23. Rosenfeld, Y. Excess-entropy and freezing-temperature scalings for transport coefficients: Self-diffusion in Yukawa systems. *Phys. Rev. E* **2000**, *62*, 7524–7527. [CrossRef]
24. Rosenfeld, Y. Quasi-universal melting-temperature scaling of transport coefficients in Yukawa systems. *J. Phys. Condens. Matter* **2001**, *13*, L39–L43. [CrossRef]
25. Ohta, H.; Hamaguchi, S. Molecular dynamics evaluation of self-diffusion in Yukawa systems. *Phys. Plasmas* **2000**, *7*, 4506–4514. [CrossRef]
26. Costigliola, L.; Pedersen, U.R.; Heyes, D.M.; Schrøder, T.B.; Dyre, J.C. Communication: Simple liquids' high-density viscosity. *J. Chem. Phys.* **2018**, *148*, 081101. [CrossRef] [PubMed]
27. Khrapak, S. Practical formula for the shear viscosity of Yukawa fluids. *AIP Adv.* **2018**, *8*, 105226. [CrossRef]
28. Khrapak, S.A.; Khrapak, A.G. Transport properties of Lennard-Jones fluids: Freezing density scaling along isotherms. *Phys. Rev. E* **2021**, *103*, 042122. [CrossRef] [PubMed]
29. Khrapak, S.A.; Khrapak, A.G. Freezing Temperature and Density Scaling of Transport Coefficients. *J. Phys. Chem. Lett.* **2022**, *13*, 2674–2678. [CrossRef] [PubMed]
30. Khrapak, S.; Khrapak, A. Freezing density scaling of fluid transport properties: Application to liquified noble gases. *J. Chem. Phys.* **2022**, *157*, 014501. [CrossRef]
31. Khan, S.U.; Ali, H.M. Swimming of gyrotactic microorganisms in unsteady flow of eyring Powell nanofluid with variable thermal features: Some bio-technology applications. *Int. J. Thermophys.* **2020**, *41*, 1–19. [CrossRef]
32. Paredes, X.; Lourenco, M.J.; Castro, C.N.D.; Wakeham, W. Thermal conductivity of ionic liquids and IoNanofluids. Can molecular theory help? *Fluids* **2021**, *6*, 116. [CrossRef]
33. Nosenko, V.; Zhdanov, S.; Pustylnik, M.; Thomas, H.M.; Lipaev, A.M.; Novitskii, O.V. Heat transport in a flowing complex plasma in microgravity conditions. *Phys. Plasmas* **2021**, *28*, 113701. [CrossRef]
34. Peng, W.; Chandra, A.; Keblinski, P.; Moran, J.L. Thermal transport dynamics in active heat transfer fluids (AHTF). *J. Appl. Phys.* **2021**, *129*, 174702. [CrossRef]
35. Zhao, A.Z.; Wingert, M.C.; Chen, R.; Garay, J.E. Phonon gas model for thermal conductivity of dense, strongly interacting liquids. *J. Appl. Phys.* **2021**, *129*, 235101. [CrossRef]
36. Chen, G. Perspectives on molecular-level understanding of thermophysics of liquids and future research directions. *J. Heat Transf.* **2022**, *144*, 010801. [CrossRef]
37. Khrapak, S.A. Vibrational model of thermal conduction for fluids with soft interactions. *Phys. Rev. E* **2021**, *103*, 013207. [CrossRef] [PubMed]
38. Khrapak, S.A. Thermal conduction in two-dimensional complex plasma layers. *Phys. Plasmas* **2021**, *28*, 010704. [CrossRef]
39. Khrapak, S.A. Thermal conductivity of strongly coupled Yukawa fluids. *Phys. Plasmas* **2021**, *28*, 084501. [CrossRef]
40. Alder, B.J.; Wainwright, T.E. Phase Transition for a Hard Sphere System. *J. Chem. Phys.* **1957**, *27*, 1208–1209. [CrossRef]
41. Smirnov, B.M. The hard-sphere model in plasma and gas physics. *Sov. Phys.-Usp.* **1982**, *25*, 854–862. [CrossRef]
42. Mulero, A. (Ed.) *Theory and Simulation of Hard-Sphere Fluids and Related Systems*; Springer: Berlin/Heidelberg, Germany, 2008. [CrossRef]
43. Pusey, P.N.; Zaccarelli, E.; Valeriani, C.; Sanz, E.; Poon, W.C.K.; Cates, M.E. Hard spheres: Crystallization and glass formation. *Philos. Trans. R. Soc. A Math. Phys. Eng. Sci.* **2009**, *367*, 4993–5011. [CrossRef] [PubMed]
44. Parisi, G.; Zamponi, F. Mean-field theory of hard sphere glasses and jamming. *Rev. Mod. Phys.* **2010**, *82*, 789–845. [CrossRef]
45. Berthier, L.; Biroli, G. Theoretical perspective on the glass transition and amorphous materials. *Rev. Mod. Phys.* **2011**, *83*, 587–645. [CrossRef]
46. Klumov, B.A.; Khrapak, S.A.; Morfill, G.E. Structural properties of dense hard sphere packings. *Phys. Rev. B* **2011**, *83*, 184105. [CrossRef]
47. Dyre, J.C. Simple liquids' quasiuniversality and the hard-sphere paradigm. *J. Phys. Condens. Matter* **2016**, *28*, 323001. [CrossRef]
48. Pieprzyk, S.; Brańka, A.C.; Heyes, D.M.; Bannerman, M.N. A comprehensive study of the thermal conductivity of the hard sphere fluid and solid by molecular dynamics simulation. *Phys. Chem. Chem. Phys.* **2020**, *22*, 8834–8845. [CrossRef] [PubMed]
49. Rao, M.R. Thermal conductivity of liquids. *Phys. Rev.* **1941**, *59*, 212. [CrossRef]
50. Hubbard, J.; Beeby, J.L. Collective motion in liquids. *J. Phys. C* **1969**, *2*, 556–571. [CrossRef]
51. Stillinger, F.H.; Weber, T.A. Hidden structure in liquids. *Phys. Rev. A* **1982**, *25*, 978–989. [CrossRef]

52. Alder, B.J.; Wainwright, T.E. Velocity Autocorrelations for Hard Spheres. *Phys. Rev. Lett.* **1967**, *18*, 988–990. [CrossRef]
53. Williams, S.R.; Bryant, G.; Snook, I.K.; van Megen, W. Velocity Autocorrelation Functions of Hard-Sphere Fluids: Long-Time Tails upon Undercooling. *Phys. Rev. Lett.* **2006**, *96*, 087801. [CrossRef]
54. Daligault, J. Universal Character of Atomic Motions at the Liquid-Solid Transition. 2020. Available online: https://arxiv.org/abs/2009.14718 (accessed on 1 October 2021).
55. Khrapak, S.; Klumov, B.; Couedel, L. Collective modes in simple melts: Transition from soft spheres to the hard sphere limit. *Sci. Rep.* **2017**, *7*, 7985. [CrossRef]
56. Bryk, T.; Huerta, A.; Hordiichuk, V.; Trokhymchuk, A.D. Non-hydrodynamic transverse collective excitations in hard-sphere fluids. *J. Chem. Phys.* **2017**, *147*, 064509. [CrossRef]
57. Yang, C.; Dove, M.T.; Brazhkin, V.V.; Trachenko, K. Emergence and Evolution of the k-Gap in Spectra of Liquid and Supercritical States. *Phys. Rev. Lett.* **2017**, *118*, 215502. [CrossRef]
58. Khrapak, S.A.; Khrapak, A.G.; Kryuchkov, N.P.; Yurchenko, S.O. Onset of transverse (shear) waves in strongly-coupled Yukawa fluids. *J. Chem. Phys.* **2019**, *150*, 104503. [CrossRef] [PubMed]
59. Kryuchkov, N.P.; Mistryukova, L.A.; Brazhkin, V.V.; Yurchenko, S.O. Excitation spectra in fluids: How to analyze them properly. *Sci. Rep.* **2019**, *9*, 10483. [CrossRef] [PubMed]
60. Khrapak, S.; Kryuchkov, N.P.; Mistryukova, L.A.; Yurchenko, S.O. From soft- to hard-sphere fluids: Crossover evidenced by high-frequency elastic moduli. *Phys. Rev. E* **2021**, *103*, 052117. [CrossRef] [PubMed]
61. Khrapak, S.A.; Yurchenko, S.O. Entropy of simple fluids with repulsive interactions near freezing. *J. Chem. Phys.* **2021**, *155*, 134501. [CrossRef] [PubMed]
62. Horrocks, J.K.; McLaughlin, E. Thermal conductivity of simple molecules in the condensed state. *Trans. Faraday Soc.* **1960**, *56*, 206. [CrossRef]
63. Bridgman, P.W. The Thermal Conductivity of Liquids under Pressure. *Proc. Natl. Acad. Sci. USA* **1923**, *59*, 141. [CrossRef]
64. Cahill, D.G.; Pohl, R. Heat flow and lattice vibrations in glasses. *Solid State Commun.* **1989**, *70*, 927–930. [CrossRef]
65. Cahill, D.G.; Watson, S.K.; Pohl, R.O. Lower limit to the thermal conductivity of disordered crystals. *Phys. Rev. B* **1992**, *46*, 6131–6140. [CrossRef]
66. Xie, X.; Yang, K.; Li, D.; Tsai, T.H.; Shin, J.; Braun, P.V.; Cahill, D.G. High and low thermal conductivity of amorphous macromolecules. *Phys. Rev. B* **2017**, *95*, 035406. [CrossRef]
67. Carnahan, N.F.; Starling, K.E. Equation of State for Nonattracting Rigid Spheres. *J. Chem. Phys.* **1969**, *51*, 635–636. [CrossRef]
68. Rosenfeld, Y. Sound velocity in liquid metals and the hard-sphere model. *J. Phys. Condens. Matter* **1999**, *11*, L71–L74. [CrossRef]
69. Khrapak, S.A. Note: Sound velocity of a soft sphere model near the fluid-solid phase transition. *J. Chem. Phys.* **2016**, *144*, 126101. [CrossRef] [PubMed]
70. Miller, B.N. Elastic Moduli of a Fluid of Rigid Spheres. *J. Chem. Phys.* **1969**, *50*, 2733–2740. [CrossRef]
71. Khrapak, S. Elastic properties of dense hard-sphere fluids. *Phys. Rev. E* **2019**, *100*, 032138. [CrossRef] [PubMed]
72. Tao, F.M.; Song, Y.; Mason, E.A. Derivative of the hard-sphere radial distribution function at contact. *Phys. Rev. A* **1992**, *46*, 8007–8008. [CrossRef]
73. Khrapak, S.A.; Khrapak, A.G. Minima of shear viscosity and thermal conductivity coefficients of classical fluids. *Phys. Fluids* **2022**, *34*, 027102. [CrossRef]
74. Lifshitz, E.; Pitaevskii, L.P. *Physical Kinetics*; Elsevier Science: Stanford, CA, USA, 1995.
75. Bell, I.H.; Galliero, G.; Delage-Santacreu, S.; Costigliola, L. An entropy scaling demarcation of gas- and liquid-like fluid behaviors. *J. Chem. Phys.* **2020**, *152*, 191102. [CrossRef]
76. Khrapak, S.A. Gas-liquid crossover in the Lennard-Jones system. *J. Chem. Phys.* **2022**, *156*, 116101. [CrossRef]
77. Pieprzyk, S.; Bannerman, M.N.; Brańka, A.C.; Chudak, M.; Heyes, D.M. Thermodynamic and dynamical properties of the hard sphere system revisited by molecular dynamics simulation. *Phys. Chem. Chem. Phys.* **2019**, *21*, 6886–6899. [CrossRef]